Med. & Biol. Eng. & Comput., 1979, 17, 742–750

Breathing ratemeter for neonatal intensive care

S. Ben-Yaakov **A. Cohen**

Electrical Engineering Department, Ben-Gurion University of the Negev, Beer-Sheva 84 120, PO Box 653, Israel

Abstract—*A new bit-to-bit ratemeter based on rate multiplication is described. The ratemeter is part of a signal monitoring and processing system used to analyse respiratory signals of neonates that are characterised by low and unstable rates. The advantages of the new ratemeter are discussed and a comparison is made with other meters. The response of the ratemeters is demonstrated by means of simulated signals as well as actual neonatal respiratory signals.*

Keywords—*Apnoea, Breathing, Ratemeters, Respiration rate*

1 Introduction

NEONATAL intensive-care units have recently received much attention in terms of monitoring and processing equipment. The availability of microprocessors and new noninvasive techniques, such as the transcutaneous pO_2 measurement (EBERHARD *et al.*, 1975), allows the continuous monitoring and processing of various physiological signals from infants (ROLFE, 1975). In contrast with intensive-care units for adults, neonatal intensive care requires an extensive monitoring and processing of respiratory signals. The respiratory system undergoes a complex transition between intra- and extra-uterine states during the birth process. Even after the first breaths of life have established independent respiration, the neonatal respiratory system remains, for a time, a system that may be inherently unstable in its ability to maintain a constant lung volume (NELSON, 1976). Infants, and especially premature infants, may develop respiratory problems that require monitoring, and, often, intervension. A common type of breathing for such infants is the 'periodic breathing', where short nonbreathing periods (apnoeas) exist. The effects of the duration and frequency of these apnoeic attacks are not exactly known. It is generally recognised, however, that a long-duration apnoea (of the order of 20 s) reflects a clinical abnormality often requiring intervension. The most common respiration monitoring device in neonatal intensive-care units is, therefore, the apnoea detector. This device detects long nonbreathing periods and activates an alarm. Recently, several investigators have suggested that multiple apnoeas of shorter duration may also have clinical implications. The cumulative affect of such apnoeas on the pulmonary arterial pressure and right ventricular failure was stressed, for example, by COCCAGNA *et al.* (1972). Several reports linking the high incidence of apnoeas with the sudden infant death syndrome have been reported (STEINSCHNEIDER, 1972).

The monitoring and processing of the respiratory signal is also important for the determination of the state of consciousness of the newborn, and especially the preterm infant. The sleep cycle, namely the total amount of sleep and the distribution of quiet and active sleep, may be important for the early development of the immature brain (GABRIEL, 1977; HOPPENBROUWERS, 1977; PRECHTL *et al.*, 1973). Many types of respiration monitoring devices have been used. These are divided into two major groups. The contactless systems include the air-filled-mattress device (LEWIN, 1969), under-mattress pressure-sensing devices (Health Devices, 1974), magnetometer devices (ROLFE, 1971), capacitance-change detectors (BARROW and COLGAN, 1973) and radar reflection systems (LIN, 1977). The contact systems include whole-body plethysmography (CROSS, 1949), pneumotachography (BLUMFIELD *et al.*, 1973), impedance pneumography (HILL *et al.*, 1967) and thermistor anemometry. A comprehensive discussion of these systems, their advantages and disadvantages, is given elsewhere (Health Devices, 1974; ROLFE, 1975; FRANKS *et al.*, 1976).

Modern neonatal intensive-care units call for more sophisticated respiration signal processing than the common apnoea detectors (Health Devices, 1974). Factors such as the respiratory rate, distribution of apnoeas and analysis of breathing modes are required. This paper describes an analogue breathing ratemeter that is used as a stand-alone monitoring device or as a part of a larger sophisticated system. The breathing signal is provided by a nasal thermistor. This sensor was chosen because of its simplicity and because most of the work was performed on premature newborns where breathing is said to be predominantly through the nose (PRECHTL

First received 4th January and in final form 23rd March 1979

0140–0118/79/060742–09 $01·50/0

et al., 1968). Any of the other respiratory sensing techniques can, of course, be used with the system.

2 Design consideration

Conventional ratemeters fall into one of two categories: (*a*) average ratemeters and (*b*) instantaneous ratemeters. By definition, average ratemeters are designed to produce an output signal e_0 that is related to the input pulse rate N_i (assumed to be constant) by

$$e_0 = K_a \int_{t}^{t+\Delta t} N_i \, dt \quad \ldots \quad (1)$$

where K_a is a proportionality constant and Δt is the integration time.

The function of an average ratemeter could be accomplished by direct digital counting over a fixed period of time, or by the diode-pump method (EARNSHAW, 1956). A close examination of these methods reveals, however, that an accurate estimation of the measured rates could be obtained only if relatively long averaging times are employed. This could be inferred by considering the relationship between the input pulse rates and the output signals of these ratemeters.

For the digital counting method, assuming a constant rate N_i, the relative percentage error ε_i in the estimate of the average rate is bounded by

$$\varepsilon_i \leqslant \frac{100}{N_i \, \Delta t_c} \quad \ldots \quad (2)$$

where Δt_c is the averaging (counting) period. Hence, for a given error ε_i, the required averaging time, is given by

$$\Delta t_c = \frac{100}{N_i \, \varepsilon_i} = \frac{100}{\varepsilon_i} T_i \quad \ldots \quad (3)$$

where T_i is the period of the incoming pulses.

The condition is not much different for the diode-pump ratemeter. Using the relationships given by BROWN (1968), we derive an expression relating the percentage ripple ε_{r_p} to the integration time constant RC and the input rate N_i

$$\varepsilon_{r_p} \leqslant \frac{100}{N_i \, CR} \quad \ldots \quad (4)$$

The step response of the diode-pump ratemeter to a change in N_i is presented by

$$e_0 = K_p(1 - e^{-t/RC}) \quad \ldots \quad (5)$$

where K_p is a constant of the system.

By combining eqns. 4 and 5 we obtain

$$e_0 = K_p(1 - \exp(-t\varepsilon_{r_p} N_i/100)) \quad \ldots \quad (6)$$

where ε_{r_p} denotes now the maximum ripple.

Assuming that the reading after a period of three time constants (95% of the final value) is accepted as a stable reading, we obtain

$$\Delta t_p = \frac{300}{\varepsilon_{r_p} N_i} = \frac{300}{\varepsilon_{r_p}} T_i \quad \ldots \quad (7)$$

where Δt_p is the reaction time of the diode-pump ratemeter.

The error parameters ε_i of the counter-type ratemeter and the ε_{r_p} of the diode-pump ratemeter specify the percentage fluctuation of the ratemeter's output for a constant N_i. To keep the fluctuations below a given value of ε_i, the counting time of the counter-type ratemeter should be at least Δt_c. This period is also the worst-case step-response time to reach the final value within ε_i. If maximum fluctuations are to be kept below, say, 5% the worst-case step-response time would thus be $20T_i$. For respiration rates of 1 pulse/s this would amount to 20 s, which, of course, is prohibitive from a practical point of view. Furthermore, since the respiration signal is nonstationary, such long averaging periods will mask important information related to the short-term perturbation in the breathing rate.

The situation is even worse for the direct diode-pump ratemeter. The present analysis indicates that the step response is about three times longer than the step response of the counter ratemeters for a given percentage fluctuation, i.e. $\varepsilon_{r_p} = \varepsilon_i$. Hence, considering the inherently slow and often unstable nature of adult and neonate respiration, one has to conclude that average ratemeters of conventional design are of little practical use in this application.

The second type of conventional ratemeter, the instantaneous ratemeter, determines the rate from the period between each two consecutive pulses. As such, these ratemeters must include a means for performing a division, since the rate is reciprocally related to the period. A number of approaches have been described for realising this calculation. They include:

(*a*) a switching time analogue divider (BROWN, 1968)

(*b*) a digital divider (ELINGS and HOLLY, 1972; SMALLWOOD, 1978)

(*c*) an analogue divider (PARVIAINEN *et al.*, 1978)

(*d*) analogue division based on hyperbolical charge, or discharge, of a capacitor (CISEK, 1972; COUSIN and SMITH, 1978).

Each of these approaches produces an analogue or a digital output and necessitates the implementation of an extra convertor to obtain the other type output. This is a disadvantage, since, in practice, both digital and analogue outputs are desirable. For a quick look and for visual recording an analogue output is desirable, whereas a digital output is preferred when digital data processing is applied. Another major drawback of the conventional instantaneous ratemeters is the fact that they offer no smoothing of the rate; i.e. the rate is calculated for every input pulse and strobed into the display section, which is thus updated from pulse to pulse. For unstable or non-stationary rates, such as could be the case in respiration rates, this mode of display could be annoying, owing to the sudden 'jumps' from one value to the other. In an analogue instantaneous ratemeter, smoothing, or averaging, could be accomplished by a damping capacitor at the output (CISEK, 1972), but they do not produce a signal that can be easily digitised.

The design of the respiration ratemeter of this study attempts to overcome some of the inherent disadvantages of previously described ratemeters. In particular, we attempted to devise a fast reacting system that produced digital and smooth analogue outputs. From the analysis given above, it was obvious that the main design difficulties are due to the fact that respiration rates are low.

This problem was overcome in the present study by applying the concept of rate multiplication. In this approach, the incoming rate is multiplied by a constant factor to produce a much higher rate. The higher rate is then processed by a diode-pump ratemeter to produce an analogue output and by a digital counter to produce a digital output.

3 General description

The system (Fig. 1) comprises five major subunits

(*a*) the front end, which includes a signal conditioner and a squaring amplifier

(*b*) the rate multiplier

(*c*) the digital output section

(*d*) the analogue output section

(*e*) the apnoea alarm section.

The input signal from the transducer (thermistor, in this case) is amplified and filtered by the signal conditioner and fed to a Schmitt trigger amplifier to produce a square wave at the basic input rate. The squared signal is fed to a pulser that produces a short pulse of a standard amplitude and constant duration, which is fed to an *RC* network. Hence, for each incoming pulse, the capacitor network is charged to a constant voltage V_{RC} and discharges towards zero voltage until the next pulse arrives. The minimum voltage e_{min} across the *RC* network will thus be

$$e_{min} \simeq V_{RC}(1-e^{-T_i/RC}) \quad . \quad . \quad . \quad . \quad . \quad . \quad (8)$$

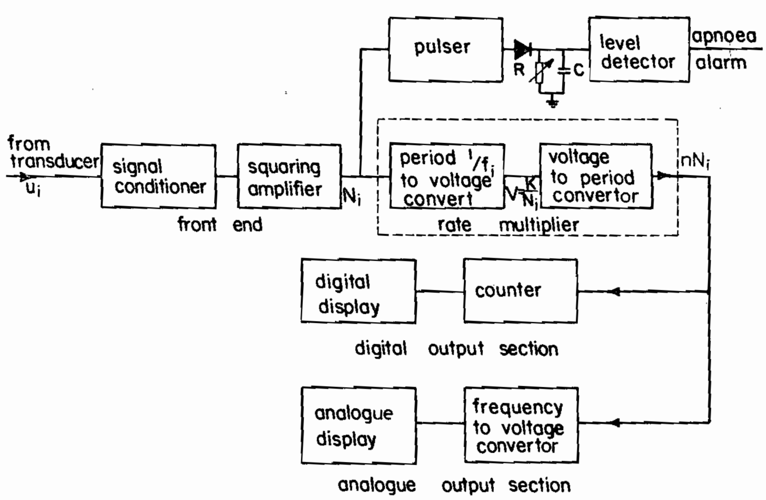

Fig. 1 Respiration ratemeter and apnoea monitor. The time constant RC determines the maximum period (lowest rate) of no-alarm

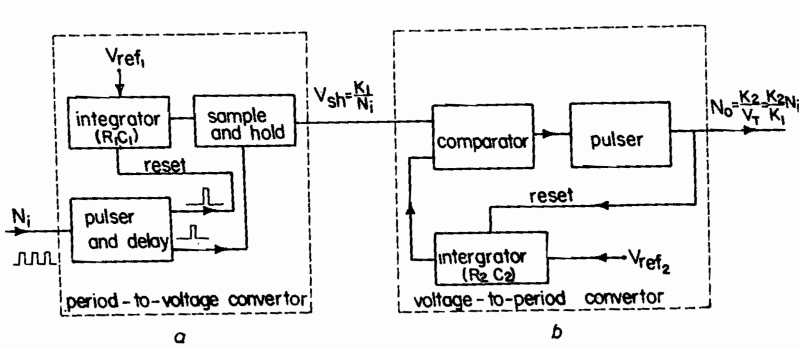

Fig. 2 Frequency multiplier: (a) Period-voltage convertor (b) Voltage-period convertor

This voltage is sensed by the level detector (Fig. 1), which produces an output whenever e_{min} drops below a given level V_L; i.e. the apnoea alarm will be activated for

$$T_i > RC \ln \left(\frac{V_{RC}}{V_{RC} - V_L} \right) \quad . \quad . \quad . \quad . \quad . \quad (9)$$

namely, when the time T_i between two successive breaths is longer than a predetermined value. By making R variable (Fig. 1), the minimum apnoea duration for an alarm can be adjusted.

The squared input signal is also fed to a rate multiplier, which first produces a voltage proportional to the pulse-pulse period and then produces a new pulse train whose period ($1/f$) is linearly related to that voltage. Consequently, the output train has a rate that is higher than the input rate by a constant factor. A more detailed description of the operation of the multiplier is given below.

Once the input rate is upscaled to yield a higher rate, signal processing continues in a conventional way. The output rate is counted by a digital counter to produce a digital output and a diode pump ratemeter is used to obtain an analogue output proportional to the rate. Since the digital section is of conventional design, no further details of this section are given here.

The principle of operation of the rate multiplier will be discussed in conjunction with Fig. 2, which depicts the basic configuration of the multiplier. The unit comprises two basic sections: (*a*) a period-voltage convertor and (*b*) a voltage-period convertor. The period measuring principle is similar to the one described by SWINNEN (1966) and used by others (BROWN, 1968; PARVIAINEN *et al.*, 1978). It basically consists of an integrator, built around an operational amplifier, which is fed by a reference voltage $V_{ref\,1}$, and followed by a sample-and-hold circuit. Each

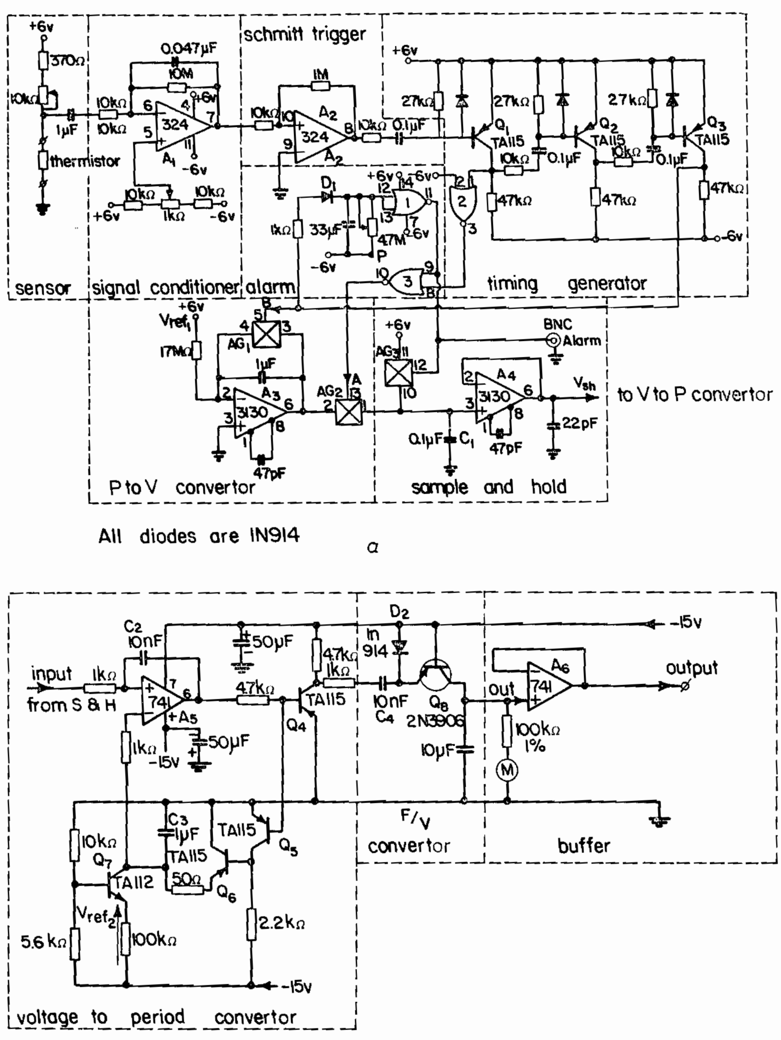

Fig. 3 *Complete circuit diagram of ratemeters and apnoea monitor (a) Signal conditioner and period-voltage convertor (b) Voltage-period convertor and frequency-voltage convertor*

incoming pulse is producing a sequence of two non-overlapping pulses; the first activates the sample and hold, which samples the output voltage of the integrator, and the second one is used to discharge the integrator's capacitor. Hence, the voltage stored by the sample and hold V_{SH} will be

$$V_{SH} = \frac{V_{ref\,1}}{R_1\,C_1\,N_i} = \frac{V_{ref\,1}}{R_1\,C_1}\,T_i \quad . \quad . \quad . \quad (10)$$

where $R_1\,C_1$ is the integration constant. The sampled voltage, which is proportional to the instantaneous period T_i of the incoming signal, is fed to a voltage-period convertor similar to the one described by BEN-YAAKOV (1969). The convertor produces a pulse train whose rate is inversely proportional to the input voltage. The convertor (Fig. 2*b*) comprises an integrator that is fed again by a constant voltage $V_{ref\,2}$, a comparator that compares the input level to the integrator output and a pulser that produces a standard pulse whenever the integrator voltage reaches the input-signal level. The pulse is used to discharge the integrator's capacitor and thus to initiate a new ramp for each incoming pulse. The period between two pulses at the output will thus be

$$T_0 = \frac{R_2\,C_2}{V_{ref\,2}}\,V_{SH} \quad . \quad . \quad . \quad . \quad . \quad . \quad . \quad . \quad (11)$$

Combining eqn. 10 with eqn. 11 we obtain

$$T_0 = \frac{V_{ref\,1}}{R_1\,C_1}\,\frac{R_2\,C_2}{V_{ref\,2}}\,T_i \quad . \quad . \quad . \quad . \quad . \quad . \quad (12)$$

or, relating the output rate N_0 to the input rate N_i

$$N_0 = nN_i \quad . \quad . \quad . \quad . \quad . \quad . \quad . \quad . \quad . \quad . \quad . \quad (13)$$

where

$$n = \frac{R_1\,C_1}{R_2\,C_2}\,\frac{V_{ref\,2}}{V_{ref\,1}} \quad . \quad . \quad . \quad . \quad . \quad . \quad . \quad . \quad (14)$$

n, the upscaling factor, can thus be set to any given number by properly choosing the parameters $R_1\,C_1$, $R_2\,C_2$, $V_{ref\,1}$ and $V_{ref\,2}$.

The analogue ratemeter used to process the output rate N_0 can now be designed according to any specific requirement. If an instantaneous respiration ratemeter is desired, the time constant (eqn. 6) of the diode-pump ratemeter is made small. If, however, a smoothing or an averaging effect is required, the time constant could be made as long as desired.

4 Circuit description

The complete circuit diagram including component values is given in Figs. 3*a* and *b*. Operational amplifier A_1 and associated components are used for the signal conditioner, which has a voltage gain of 10^3 and a bandwidth of approximately 0·5 Hz. Attenuation of the mains frequency (50 Hz in Israel) is thus about 40 dB. Following the filter amplifier is a Schmitt trigger A_2 that was designed with a 10 mV hysteresis to increase the noise immunity of the system and to improve the rise time of the output signal. The square-wave-type signal generated by the zero-crossing detector is then fed to a timing generator built around Q_1, Q_2 and Q_3. The output pulse at the collector of Q_3 is delayed with respect to the output pulse at the collector of Q_1 but the two pulses are nonoverlapping. The pulses are fed to the period-voltage convertor and to the apnoea-alarm circuit, which comprises a diode D_1, a parallel *RC* circuit and a gate NOR_1 used as a level detector. The output of the gate will switch to a high-level state when the voltage at the input is below the trigger level. Namely, the apnoea alarm will be activated when the time between two successive breaths is longer than a predetermined value as set by potentiometer P.

The capacitor of the integrator built around A_3 is discharged with every pulse of Q_3. Prior to the capacitor's discharge, the timing pulse of Q_1 activates the analogue gate AG_2 and the output voltage of the integrator is sampled by capacitor C_1. Hence, the output voltage of the buffer amplifier A_4 is proportional to the instantaneous respiration period. Since sampling is initiated at the end of the period, the output voltage will stay constant if, for some reason, the current respiration period is very long or even infinitely long. To avoid this erroneous indication, a logic circuit composed of NOR_2 and

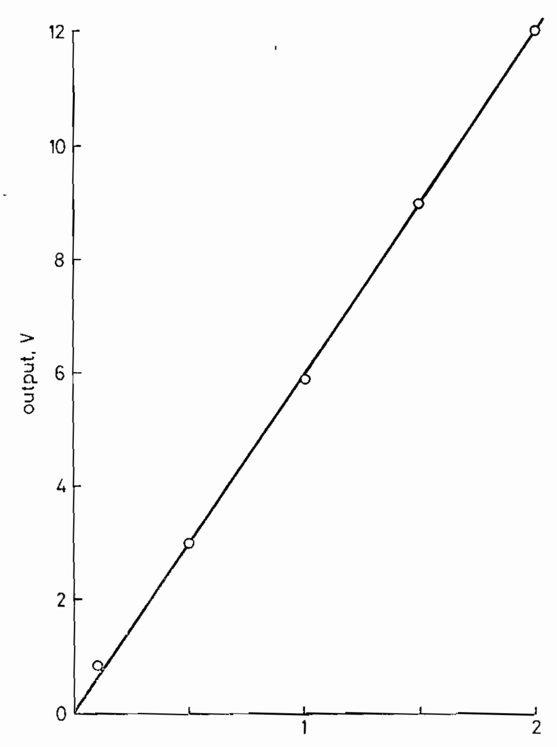

Fig. 4 Static calibration curve of respiration ratemeter

NOR_3 will discharge the sampling capacitor when the apnoea alarm is activated. Hence, during a respiration interruption, the voltage will be constant for the predetermined apnoea delay period and then drop to zero.

The output voltage of the period-voltage convertor is fed (Fig. 3*b*) to the voltage-period convertor built around A_5 and Q_4, Q_5, Q_6, Q_7 serves as a current source, charging C_3 by a constant current. When the voltage across the capacitor reaches the input level to the convertor, A_5 will switch and produce a short pulse due to the positive feedback via capacitor C_7. This pulse is level translated by Q_5 that drives the switch Q_6 used to discharge the ramp capacitor C_3. Following the pulse, the voltage across C_3 will increase linearly until it again reaches the level of the input signal to the convertor.

The rate of the output signal of the voltage-period convertor is converted to a proportional voltage level by the diode-transistor pump ratemeter. This ratemeter is more linear than the diode pump owing to the complete isolation between input and output signals. The ratemeter is constructed from a capacitor C_4, diode D_2 and transistor Q_8. For each pulse, C_4 is charged to approximately the supply voltage (minus the voltage drop across D_2) and discharges into the emitter of Q_8. Assuming that the current transfer ratio of the transistor α is approximately unity, the average collector current is directly proportional to the pulse rate, C_4 capacitance and supply voltage. The incremental current pulses are smoothed out by the output filter and the low ripple output is used to feed a buffer amplifier and a microammeter.

5 Results and discussion

A static calibration curve of the instrument (Fig. 4) was obtained by feeding a square-wave signal of known frequency into the input and monitoring the output. The linearity of response was found to be acceptable with a maximum deviation from a straight line of less than $1 \cdot 5\%$ of full scale. The deviation of the low-frequency data point

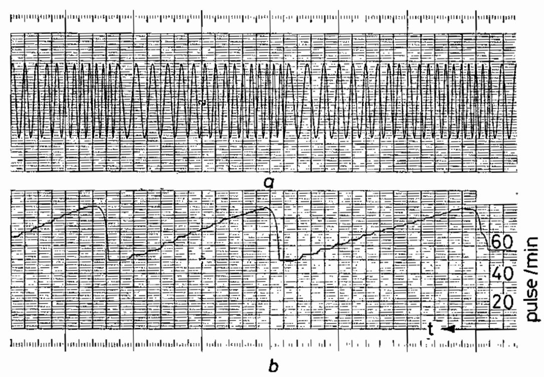

Fig. 5 (a) Input signal, sinewave with approximated sawtooth frequency modulation in the range of 0·84 to 1·48 Hz (b) Output of ratemeter, recording speed 5 mm/s

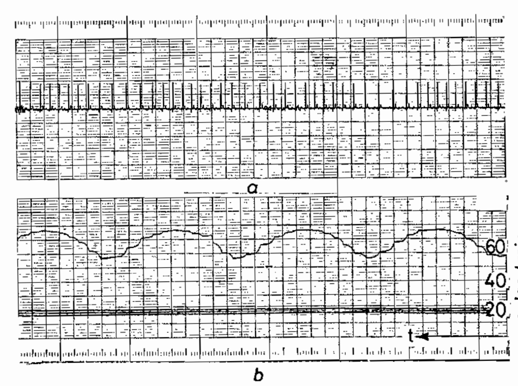

Fig. 7 (a) Simulated e.c.g. with sinusoidal R-R interval (b) Output of ratemeter, recording speed 5 mm/s

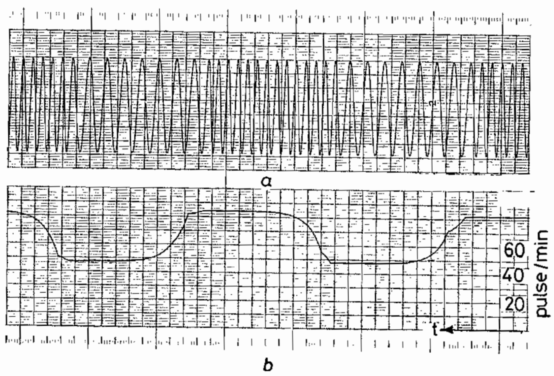

Fig. 6 Step response of system: (a) Input signal, sinewave frequency modulated by a square wave (b) Output of ratemeter, recording speed 5 mm/s

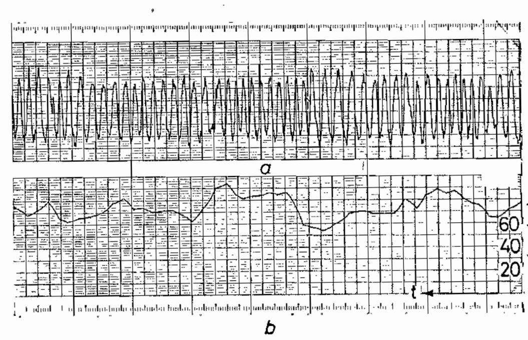

Fig. 8 Breathing of premature infant during quiet sleep (a) Breathing signal (b) Output of ratemeter recording speed 5 mm/s

(0·1 Hz) from the straight line of Fig. 4 is probably due to the leakage of transistor Q_8 and the bias current of A_6 (Fig. 3*b*), which become significant when the signal current is small. Another possible source of error is the leakage currents and voltage offsets of the period-voltage convertor and sample-and-hold circuit (Fig. 2*a*). However, frequencies below 0·1 Hz (6 pulses/min) are of no interest here, as the system is designed to activate the apnoea alarm if the period between two breaths is longer than about 10 s. When the apnoea alarm is activated, the output signal is forced to zero.

The conversion factor of the frequency multiplier of the present instrument was set to about 400. The maximum output frequency is thus approximately 800 Hz, corresponding with a respiration rate of 120 pulses/min. The analogue output voltage was adjusted to 12 V at full scale (Fig. 4) corresponding to a conversion factor of 0·1 V per pulses/min referred to the input signal rate.

The dynamic response of the instrument was checked by means of simulated data. A frequency modulated sinewave (Fig. 5), the frequency of which was slowly changed by hand, was used to simulate sawtooth modulation. The bit-to-bit updating of the rate output is clearly seen at the output of the ratemeter (Fig. 5). The output 'ripple' noise increases with decreasing frequency, having a value of about 0·2 pulses/min for the lower, one cycle, frequency. Fig. 6 demonstrates the step response of the instru-

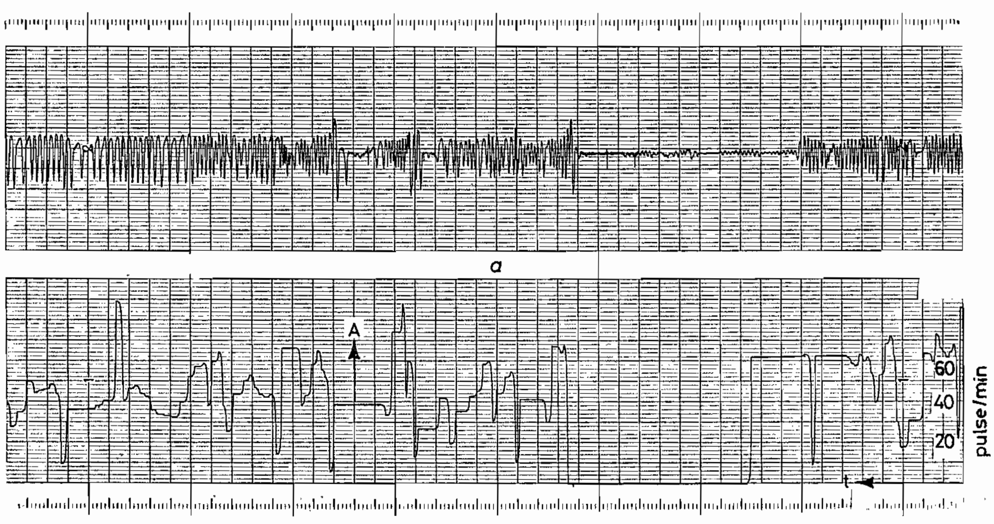

Fig. 9(i) Breathing of premature infant during active sleep (a) Breathing signal (b) Output of ratemeter, recording speed 1 mm/s

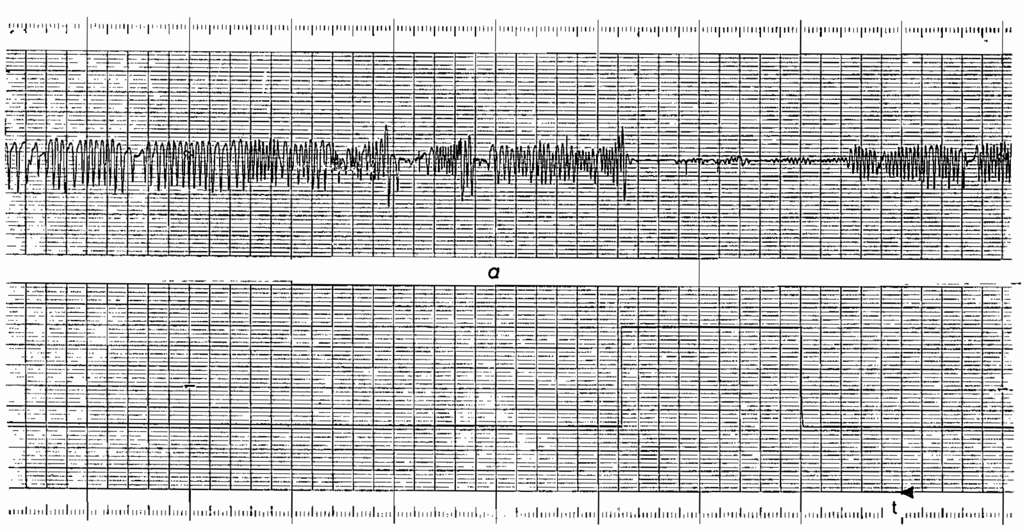

Fig. 9(ii) Apnoea alarm output [same signal as in Fig. 9(i)] ment. For these frequencies, a steady-state reading is reached after about three pulses. A simulated e.c.g. signal with sinusoidal R-R interval modulation is shown in Fig. 7.

A sample of respiratory rate monitoring from a premature infant is shown in Figs. 8–9. Fig. 8 demonstrates a breathing record during quiet sleep. The record displays a regular respiration with slow varying rates in the range of 60 to 90 pulses/min. Fig. 9*a* depicts 'periodic breathing' recording from the same infant, during active sleep. This breathing is characterised by 'non breathing' periods of various durations. In this active sleep example breathing rates vary drastically, to cover the range of 0 to 90 pulses/min. A long period of more than 50 s with only very shallow respiration is seen in the record. The instrument's threshold level was so adjusted that it did not recognise the small fluctuations as breathings and considered the complete 50 s period as an apnoea. The alarm was activated about 12 s after the initiation of the apnoea, and was shut off approximately 3 s after initiation of breathing, as shown in Fig. 9*b*. During the apnoea period the rate is set to zero. Note, however, that for the initial 10 s period of the apnoea, the rate was held at a constant value of 62, which was the rate just before the apnoea incident. This is the case, since the lowest rate recognised by the system is 6 pulses/min. The corresponding 10 s 'hold' time is required in order to search for the next incoming pulse. This property somewhat distorts the resultant rate record; e.g. consider the section denoted by 'A' in Fig. 9*a*. This section shows a plateau of 12 s with rate value of 38 and a short period of about 1 s, having the rate value of 5 pulses/min. Observing the corresponding breathing record, the correct duration of the lower rate signal was 'masked' by the search time and thus appeared to be shorter, while the previous reading was made longer. This phenomenon is better demonstrated in the simulated signal shown in Fig. 10. In Fig. 10*a* the frequency of a sinewave was switched from 1 Hz to 0·01 Hz every 15 s. The true rate of the signal is a square wave with amplitudes of 60 and 0·6 pulses/min in 15 s duration. Fig. 10*b* demonstrates the improvement as the lower rate increases.

The 'holding distortion' is a direct consequence of the instantaneous ratemeter method. Since readings are obtained at the end of the cycle, the current reading of an instantaneous ratemeter always corresponds to the preceding cycle. This phenomenon is especially noticeable when the current period is appreciably longer than the preceding period, as demonstrated in Fig. 10.

The performance of the present instrument seems to suggest that frequency multiplication could be a useful approach for monitoring very low frequency rates. The static and dynamic response of the ratemeter have been tailored for the specific application on hand: monitoring the breathing of premature infants. Other applications may require a somewhat different response that could be obtained by minor changes in the electronic circuit. The one cycle delay between the reading of the ratemeter and the current cycle is, however, inherent to the method of instantaneous ratemeter. This delay may cause some confusion when the current period is very long compared with the preceding one. In this case the instrument will display the instantaneous rate of the previous (short) period during the current (long) period until the reading is updated at the end of the cycle. This difficulty could be partially overcome by some additional circuitry that will compare the current output of the period-voltage convertor to the maximum value reached at the previous cycle. If the current period is longer, i.e. the instantaneous voltage

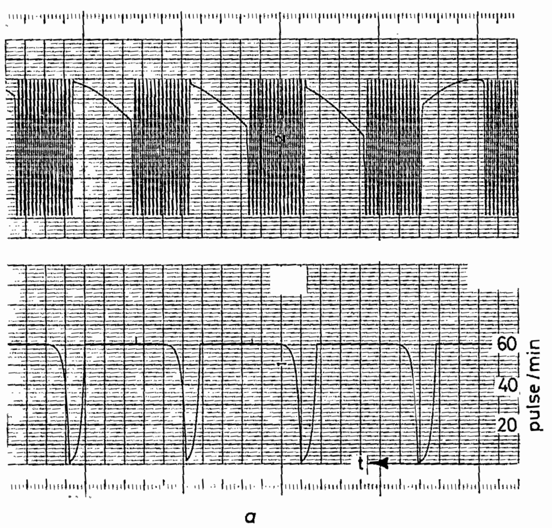

a

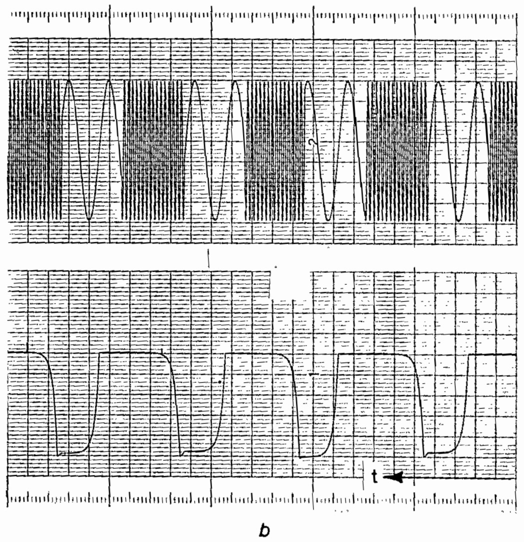

b

Fig. 10 Response of ratemeter to a change in input rate. See text for discussion, recording speed 1 mm/s of the time-voltage convertor is higher than the preceding maximum, the sample-and-hold gate (AG_2 in Fig. 3*a*) will be opened. This will cause the output voltage to decay hyperbolically toward the value reached at the end of the current cycle.

References

BARROW, R. E. and COLGAN, F. J. (1973) A non-invasive method for measuring newborn respiration. *Respiratory Care*, **18**, 412–414.

BEN-YAAKOV, S. (1969) Analog-to-period converter can simplify telemetry systems. *Electronic Design*, **17**, 240–241.

BROWN, B. H. (1968) Low-frequency-averaging and instantaneous ratemeters. *Electronic Engr.*, **40**, 2–5.

BLUMFIELD, W., TURNEY, S. and COWLEY, R. A. (1973) Mathematical model for flow in the heated fleisch pneumotachometer. *Med. & Biol. Eng.*, **11**, 546–551.

CISEK, A. (1972) A new design for a linear, pulse-to-pulse and mean frequency cardiotachometer. *Med. & Biol. Eng.*, **10**, 89–91.

COCCAGNA, G., MANTOVANI, M., BRIGNANI, F. *et al.* (1972) Continuous recording of the polymunary and systematic arterial pressure during sleep in syndromes of hypersomnia with periodic breathing. *Bull. Physiopathol.*, **8**, 1159–1163.

COUSIN, A. J. and SMITH, K. C. (1978) Instantaneous cardiac tachometer with extendable range. *Med. & Biol. Eng. & Comput.*, **16**, 379–382.

CROSS, K. W. (1949) The respiratory rate and ventilation in the newborn baby. *J. Physiol.*, **109**, 459.

EARNSHAW, J. B. (1956) The diode pump integrator. *Electronic Engr.*, **36**, 26.

EBERHARD, P., MINDT, W., JANN, F. and HAMMACHER, K. (1975) Continuous pO_2 monitoring in the nenonate by skin electrodes. *Med. & Biol. Eng.*, **13**, 436–442.

ELINGS, V. and HOLLY, D. (1973) A cardiotachometer which calculates rate digitally. *IEEE Trans.*, **BME-20**, 468–470.

FRANKS, C. I., BROWN, B. H. and JOHNSTON, D. M. (1976) Contactless respiration monitoring of infants. *Med. & Biol. Eng.*, **14**, 306–312.

GABRIEL, M. and ALBANI, M. (1977) Rapid eye movement sleep, apnoea and cardiac slowing influenced by phenobarbital administration in the nenoate. *Pediatrics*, **60**, 426–430.

HEALTH DEVICES (1974) Emergency care research inst.: infant apnoea monitors, *Health Devices*, **4**.

HILL, R. V., JANSEN, J. C., FLING, J L (1967) Electrical impedance plethysmography: a critical analysis. *J. Appl. Physiol.*, **22**, 161–168

HOPPENBROUWERS, T., HODGMAN, J. E., HARPER, R. M. *et al.* (1977) Polygraphic studies of normal infants during the first six months of life. III. Incidence of apnoea and periodic breathing. *Pediatrics*, **60**, 418–425.

LEWIN, J. E. (1969) An apnoea-alarm mattress. *Lancet*, Sept. II, 667–668.

LIN, C. J., DAWE, E. and MAJCHEREK, J. (1977) A non-invasive microwave apnoea detector. *Proc. San Diego Biomed Symp.*, **16**, 441–443.

NELSON, N. M. (1976) Respiration and circulation after birth. *In* SMITH, C. A. and NELSON, N. M. (Eds.) *The physiology of the newborn infant*, C. C. Thomas, Springfield, Ill., 4th edition.

PARVIAINEN, T., HAKUMAKI, M. and HALINEN, M. (1978) Ratemeter based on analogue divider. *Med. & Biol. Eng. & Comput.*, **16**, 1121–1123.

PRECHTL, H. F. R., AKIYAMA, Y., ZINKIN, P. and GRANT, D. K. (1968) Polygraphic studies of the full term newborn (technical aspects and quantitative analysis) in studies in infancy. *In* MACKEITH, R. and BAX, M. (Eds.) *Clinics in Developmental Medicine*, No. *27*.

PRECHTL, H. F. R., THEORELL, K. and BLAIR, A. W. (1973) Behavioural state cycles in abnormal infants. *Devel. Med. Child Neural.*, **15**, 606–615.

ROLFE, P. (1971) A magnetometer respiration monitor for use with premature babies. *Biomed. Engr.*, **6**, 402–404.

ROLFE, P. (1975) Monitoring in newborn intensive care. *Biomed. Engr.*, **10**, 399–404.

SMALLWOOD, R. H. (1978) An instantaneous ratemeter for low frequency signals. *Electronic Engr.*, **60**, 27.

STEINSCHNEIDER, A. (1972) Prolonged apnoea and the sudden infant death syndrome, clinical and laboratory observations. *Pediatrics*, **50**, 646–668.

SWINNEN, M. E. (1966) A novel cardiotachometer. *IEEE Trans.*, **BME-13**, 100–101.